Shock-Tube Study of the Oxidation of Acetaldehyde at High Temperature

Seok-Jae Won, Ji-Cheol Ryu, Jun-Hyun Bae,† Youn-Doo Kim, and Jun-Gill Kang*

Department of Chemistry, Chungnam National University, Taejon 305-764, Korea
†Department of Environmental Engineering, Anyang University, Kyungki-Do 430-714, Korea
Received March 3, 2000

The combustion characteristics of a mixture of acetaldehyde, oxygen and argon behind a reflected shock wave at temperatures ranging from 1320 to 1897 K at 100 torr were studied. The emission from the OH radical at 306.4 nm and the pressure profile behind the reflected shock were measured to monitor ignition delay time. The ignition delay times were computed from a proposed mechanism of 110 elementary reactions involving 34 species. The simulation and sensitivity analysis confirms that the main channel for oxidation of acetaldehyde at high temperature consists of the Rice-Herzfeld mechanism, the decomposition and oxidation of HCO, and the reaction of H with O_2.

Introduction

The gas-phase oxidation of acetaldehyde has drawn a great deal of attention, since acetaldehyde is an important intermediate in the oxidation of many hydrocarbon fuels. Most of works on the oxidation of acetaldehyde use a static reactor[1] and a continuous-flow stirred tank reactor (CSTR).[2,3] Those systems are designed for the low-temperature combustion (T < 800 K) in order to study the autoignition conditions that produce knock in a spark-ignition engine. The low-temperature oxidation of acetaldehyde in the CSTR exhibits oscillatory cool flames and ignition. The oscillatory phenomena in the CSTR have been described using a detailed elementary reaction mechanism. Simulations of the autoignition have demonstrated that the oxidation of acetaldehyde at the low temperature is initiated via the formation of peracetic acid, which generates a branching chain reaction. Peracetic acid is also one of the important intermediates in the combustion of n-butane at low temperature.[4] The high-temperature oxidation of acetaldehyde has been investigated in a turbulent flow reactor by Colket *et al.*[5] and in a jet-stirred reactor by Dagaut *et al.*[6] The methyl and hydroxyl radicals play the major role in the oxidation of acetaldehyde in the high temperature, while alkyperoxide intermediates have been excluded from the reaction mechanism in the combustion of hydrocarbon fuels at high temperature.[7]

Up to date, a few paper dealing with the combustion of acetaldehyde behind shock wave has been published.[8,9] Daguet *et al.* also measured ignition delay times in the acetaldehyde oxidation behind the reflected shock.[6] However, a comprehensive work on the oxidation of acetaldehyde in the shock tube has not been reported. This study investigated the combustion of acetaldehyde at high temperature in detail. The ignition delay time of acetaldehyde and oxygen mixture diluted in argon was monitored behind a reflected shock by measuring pressure profile and the OH radical emission profile. The detailed kinetics of the ignition of acetaldehyde were proposed from simulations of the ignition delay time.

Experimental Section

The shock tube apparatus with a driven section of 3,100 mm long and 24.3 mm internal diameter has been described in detail elsewhere.[10,11] Test gas mixture was prepared by mixing acetaldehyde (Fukuda, 99%+), oxygen (99.9% pure) and argon (99.999% pure) manometrically within an error of ±0.1 torr and was stored in a Pyrex flask connected to the driven section of the shock tube. The gases were kept warm at *ca.* 30 °C and stirred in order to prevent the condensation of acetaldehyde. The driver gas was pure grade helium (99.999%). Eight different mixtures, as listed in Table 1, were prepared. The argon concentration was varied to examine the effect of argon on the ignition delay time.

The reflected shock parameters (T_5, P_5) were calculated

Table 1. Experimental conditions for CH_3CHO-O_2-Ar mixtures behind a reflected shock (p_1=100 torr)

Mixture	Concentration(M)/10^{-4}			Equivalence Ratio (Φ)	T_5 (K)	P_5 (atm)	τ (μs)
	CH_3CHO	O_2	Ar				
A	1.59	4.76	46.5	0.83	1320-1646	3.254-4.640	171-916
B	3.17	6.34	43.4	1.25	1358-1897	3.526-5.975	108-840
C	3.17	4.76	44.9	1.67	1414-1702	3.642-4.882	301-960
D	1.06	2.64	49.2	1.00	1372-1678	3.314-4.550	250-992
E	2.12	5.29	30.0	1.00	1314-1517	3.410-4.319	273-656
F	2.12	5.29	35.5	1.00	1399-1522	3.717-4.264	341-657
G	2.12	5.29	45.5	1.00	1342-1857	3.372-5.644	96-861
H	2.12	5.29	55.0	1.00	1455-1505	3.619-3.997	489-663

from the incident shock speed and the composition of the mixture in the driven section by using the NASA/Lewis equilibrium program. In this program, the composition of the mixture is assumed to be fixed for any thermodynamic process from the initial condition to the shocked condition.[12] The ignition delay time was simulated using the CHEMKIN package,[13] which includes thermodynamic data for chemical species considered in the mechanism. Analysis of our mechanism was also performed using KINALC package.[14]

Results and Discussion

Ignition Delay Time. Figure 1 shows a typical oscillogram of profiles of the pressure and OH emission intensity observed at the end of the driven section. The signals were triggered simultaneously when the incident shock wave passed through a pressure transducer installed at 255 mm from the end plate. The arrival of the reflected shock induced a mild pressure rise, followed by a sharp pressure spike, which is associated with the ignition. At the same time, a sudden increase in the OH emission is observed. The ignition delay time, τ, is defined as the period between the arrival of the reflected shock and the maximum OH emission intensity. The ignition delay time derived from the pressure profile is the same as that derived from the OH emission. It is worth noting that a typical pressure oscillogram could not be obtained from the mixture with more than 95% Ar. In this study, we confined our attention to mixtures with less than the 95% Ar. The range of the observed ignition delay times and the reflected shock temperature (T_5) for each mixture are also listed in Table 1.

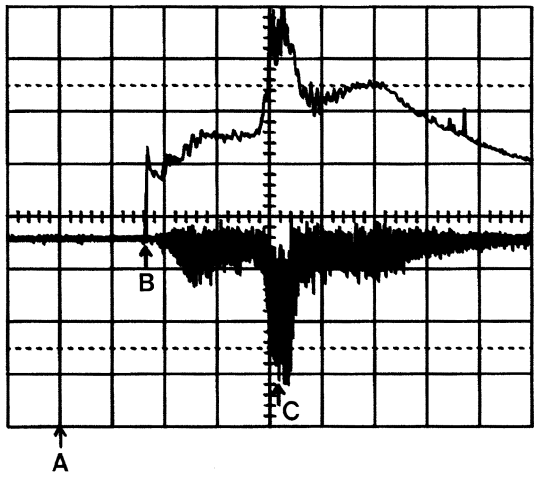

Figure 1. Typical oscillograme of pressure (upper) and 306.4 nm emission intensity (lower) profiles in CH_3CHO-O_2-Ar mixture behind a reflected shock (A: point triggered by an incident wave B: an arrival of a reflected shock and C: onset of detonation). The sweep speed is 0.2 ms/div.

The plot of $ln\ \tau$ *vs.* $1/T_5$ is very useful for formulating observed ignition delay times thermodynamically. In Figure 2 the relationship between $ln\ \tau$ and $1/T_5$ for each mixture is quite linear. Accordingly, the observed ignition delay times

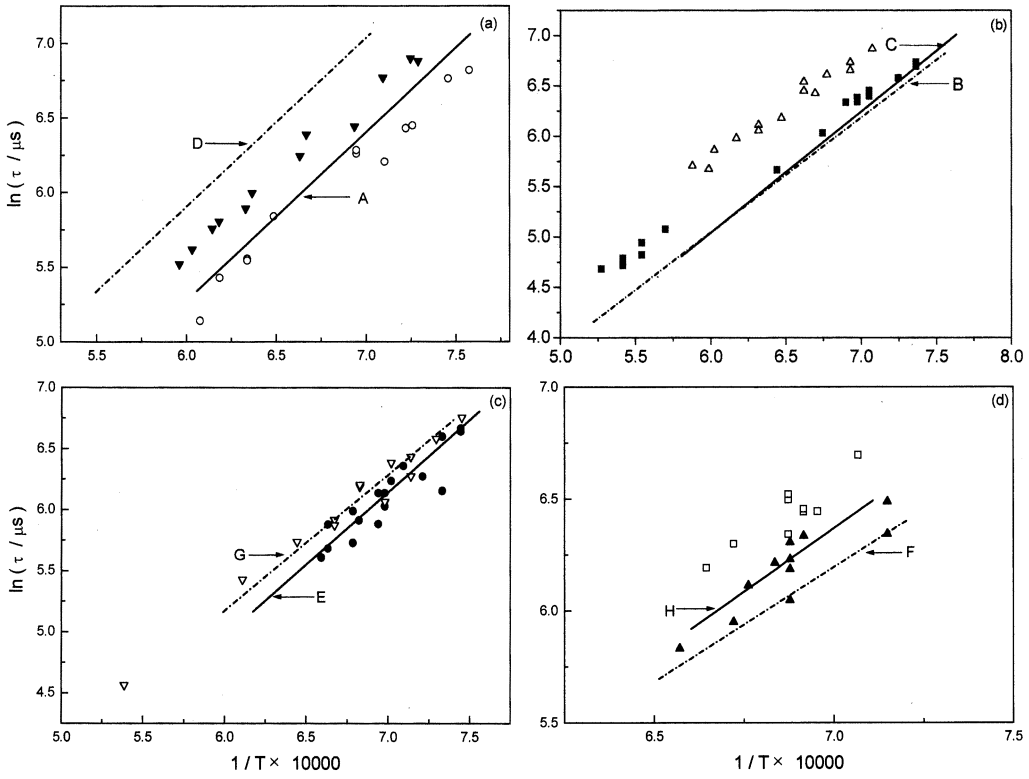

Figure 2. Plot of ln (τ/μs) *vs.* 1/T for CH_3CHO-O_2-Ar mixture: (a) A (○, 3 : 9 : 88) and D (▼, 2 : 5 : 93), (b) B (■, 6 : 12 : 82) and C (△, 6 : 9 : 85), (c) E (●, 5.7 : 14.1 : 80.2) and G (▽, 4 : 10 : 86), and (d) F (▲, 5 : 12.5 : 82.5) and H (□, 3.4 : 8.5 : 88.1). The lines represent calculated values for the corresponding mixtures.

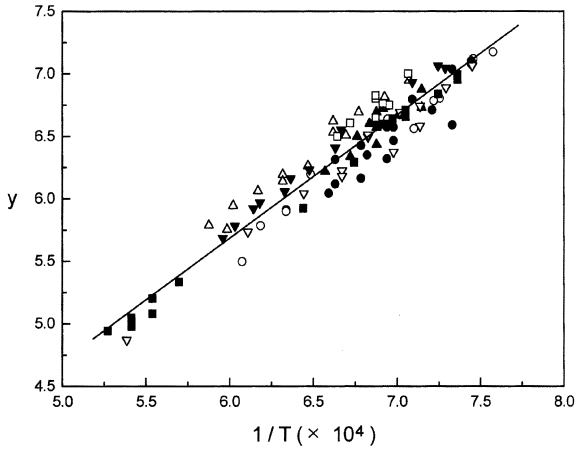

Figure 3. Plot of y *vs.* $1/T$ for CH_3CHO-O_2-Ar mixture: A (○, 3 : 9 : 88), B (■, 6 : 12 : 82), C (△, 6 : 9 : 85), D (▼, 2 : 5 : 93), E (●, 5.7 : 14.1 : 80.2), F (▲, 5 : 12.5 : 82.5), G (▽, 4 : 10 : 86) and H (□, 3.4 : 8.5 : 88.1), where $y = ln\{\tau/(1.584 \times 10^{-6} [CH_3CHO]^{0.41} [O_2]^{-0.58} [Ar]^{0.31})\}$.

can be fitted to an Arrehenius formula

$$\tau = \boldsymbol{A} \exp(\boldsymbol{E}/\boldsymbol{RT_5}) [CH_3CHO]^a [O_2]^b [Ar]^c$$

where $\boldsymbol{A}$ is the pre-exponential factor, $\boldsymbol{E}$ is an activation energy, and a, b and c are reaction orders. Multiple regression analysis was employed to obtain the best-fit parameters. The final results are

$$\tau = 1.584 \times 10^{-6} \exp(\boldsymbol{E}/\boldsymbol{RT_5}) [CH_3CHO]^{0.41} [O_2]^{-0.58} [Ar]^{0.31}$$

$$E = 18.62 \text{ kcal·mol}^{-1} (\pm 0.61 \text{ kcal·mol}^{-1})$$

where τ and concentration are given in s and mol dm^{-1}. The reliability of these results can be tested by plotting all data as $ln\{\tau/(1.584 \times 10^{-6} [CH_3CHO]^{0.41} [O_2]^{-0.58}[Ar]^{0.31})\}$ *vs.* $1/T_5$. As shown in Figure 3, all the points lie close to a single line, the slop of which represents the value of E/R.

The observed activation energy of acetaldehyde is very low, compared with the reported values for some compounds. The observed vale is higher that that of acetylene (14.7 kcal·mol^{-1})[11] but is comparable with that of ethylene oxide (19.3 kcal·mol^{-1}).[16] Previously, we reported the theoretical values for the activation energies and energy changes for the decomposition of ethylene oxide.[10] The conformational energy of acetaldehyde is 30.46 kcal·mol^{-1} higher than that of ethylene oxide. Therefore, the combustion of ethylene oxide should be more exothermic than that of its isomer, acetaldehyde. However, the activation energy of the two isomers is almost the same. It should be noted that under similar experimental conditions, the acetaldehyde mixtures produced much longer delay times than ethylene oxide. For the equivalent-ratio mixture (diluted in Ar with *ca.* 85% mole ratio) at T_5=1430 K, the delay time was observed to be *ca.* 670 μs for the acetaldehyde mixture and *ca.* 60 μs[10] for the ethylene oxide mixture. Provisionally, it is assumed that the reactivity between the isomers is related to the induction period rather than the activation energy. Argon inhibits the oxidation of acetylene and ethylene oxide, although in the acetaldehyde oxidation the Ar content has a negligible effect on the ignition delay time compared with the effects of acetaldehyde and oxygen.

Simulating the Ignition Delay Time. Experimental and modeling studies of acetaldehyde oxidation have been focused on low temperature phenomena.[3] Below 500 K, H-atom abstraction by molecular oxygen is the major initiation step and the propagation steps involve formation of acetylperoxyl radical *via* O_2 addition:

$$CH_3CHO + O_2 = CH_3CO + HO_2$$

$$CH_3CO + O_2 = CH_3CO_3$$

In the chain branching reaction, the acetylperoxide radical accelerator forms *via* the formation of peracetic acid:

$$CH_3CO_3 + CH_3CHO = CH_3CO_3H + CH_3CO$$

$$CH_3CO_3H = CH_3 + OH + CO_2$$

As temperature increases above 500 K, the rate of the decomposition of acetyl radical increases relative to the addition of O_2:

$$CH_3CO + M = CH_3 + CO + M \quad (10)$$

Cavanagh *et al.*[3] proposed the detailed mechanism of acetaldehyde oxidation at low temperature that involves methylperoxy and acetylperoxyl reactions. Initially, we considered their mechanism to calculate the ignition delay time. However, the calculated ignition times were not close to the observed values. This necessitated developing a more reliable kinetic scheme to explain our observed ignition delay times in CH_3CHO-O_2-Ar mixtures behind a reflected shock. At high temperature, the channel via acetylperoxide radical was found to be insensitive to the ignition delay time. Instead, we added a fairly simple Rice-Herzfeld mechanism[16] to the reaction scheme (reactions (2), (3), (6) and (10)) as initiation and chain steps. These are well accepted for acetaldehyde pyrolysis. In addition, the H-atom abstraction of acetaldehyde was also considered as another initiating reaction:

$$CH_3CHO + M = CH_3CO + H + M \quad (1)$$

We added some reactions of methane with O_2 and small radicals to our reaction scheme, since methane may be formed from the reaction of acetaldehyde with methyl radical. The dimerization of methyl radical and its subsequent reactions, which might be additional steps, are also included in our scheme.

To fit the observed ignition delay times more precisely, the elementary steps responsible for the chemiluminescence of OH radical were incorporated into the scheme. In the premixed flame, the strong OH emission from the reaction zone of hydrocarbon flame is associated with CH oxidation.[17]

$$CH + O_2 = CO + OH^* \quad (31)$$

This reaction is very exothermic ($\Delta H = -159.3$ kcal at 1000 K) and it might provide sufficient energy to excited OH from the ground $^2\Pi$ state to the emitting $^2\Sigma$ state of OH ($U = 92.8$ kcal·mol^{-1}). In the hydrogen-oxygen reaction in shock tube

Table 2. Reaction mechanism and rate constants for CH_3CHO-O_2-Ar mixtures behind a reflected shock

No.	Reaction	*A*	*n*	E_a	ref
(1)	$CH_3CHO+M=CH_3CO+H+M$	5.00E14	0.0	88000	[19]
(2)	$CH_3CHO+M=CH_3+HCO+M$	3.00E14	0.0	80000	[19]
(3)	$CH_3CHO+H=CH_3CO+H_2$	8.00E12	0.0	4206	adjusted
(4)	$CH_3CHO+OH=CH_3CO+H_2O$	4.15E11	0.0	517	adjusted
(5)	$CH_3CHO+O_2=CH_3CO+HO_2$	5.03E13	0.0	364800	[4]
(6)	$CH_3CHO+CH_3=CH_3CO+CH_4$	2.00E-6	5.6	2464	[3]
(7)	$CH_3CHO+HO_2=CH_3CO+H_2O_2$	1.50E12	0.0	10036	[3]
(8)	$CH_3CHO+HCO=CH_3CO+CH_2O$	7.80E13	0.0	8440	[21]
(9)	$CH_3CHO+CH_3O=CH_3CO+CH_3OH$	1.37E12	0.0	3000	[4]
(10)	$CH_3CO+M=CH_3+CO+M$	2.00E10	0.0	15000	[19]
(11)	$CH_3CO+M=CH_2CO+H+M$	3.00E13	0.0	8000	[20]
(12)	$CH_2CO+O=HCO+HCO$	1.00E13	0.0	5960	adjusted
(13)	$CH_2CO+OH=CH_2O+HCO$	2.80E13	0.0	0	[22]
(14)	$CH_2CO+OH=HCCO+H_2O$	1.00E13	0.0	2630	[10]
(15)	$HCCO+H=CH_2+CO$	1.50E14	0.0	0	[21]
(16)	$HCCO+O_2=CO+CO+OH$	1.46E12	0.0	2500	[21]
(17)	$CH_4+O_2=CH_3+HO_2$	7.94E13	0.0	55887	[23]
(18)	$CH_4+O=CH_3+OH$	1.02E09	1.5	8609	[23]
(19)	$CH_4+OH=CH_3+H_2O$	1.60E06	2.1	2462	[24]
(20)	$CH_4+H=CH_3+H_2$	2.20E04	3.0	8842	[22]
(21)	$CH_4+HO_2=CH_3+H_2O_2$	2.00E13	0.0	18000	[24]
(22)	$CH_3+CH_3=M+C_2H_6+M$ H_2/2./H_2O/6./CH_4/2./CO/1.5/CO_2/2./C_2H_6/3./Ar/0.7./	2.12E16	–0.97	620	[25]
(23)	$CH_3+CH_3=C_2H_5+H$	4.99E12	0.1	10600	[25]
(24)	$CH_3+O_2=CH_3O+O$	2.68E13	0.0	28800	[25]
(25)	$CH_3+O_2=CH_2O+OH$	5.34E13	0.0	34574	[24]
(26)	$CH_3+OH=CH_2OH+H$	5.63E13	0.0	6118	[22]
(27)	$CH_3+H=CH_2+H_2$	9.00E13	0.0	15100	[22]
(28)	$CH_3+H+M=CH_4+M$ H_2O/5./CO_2/3./CO/2./H_2/2./	8.00E26	–3.0	0	[22]
(29)	$CH_3+OH=CH_2+H_2O$	7.50E06	2.0	5002.4	[23]
(30)	$CH_3+HO_2=CH_3O+OH$	2.00E13	0.0	0	[25]
(31)	$CH+O_2=CO+OH$	2.00E13	0.0	0	[4]
(32)	$CH_2+O_2=CO_2+H+H$	1.60E12	0.0	1000.1	[22]
(33)	$CH_2+CO+M=CH_2CO+M$ H_2O/5./CO_2/3./ CO/2./H_2/2./	2.76E13	0.0	–14799	[23]
(34)	$CH+H=C+H_2$	1.50E14	0.0	0	[22]
(35)	$C+OH=CO+H$	5.00E13	0.0	0	[22]
(36)	$C_2H_6+H=C_2H_5+H_2$	1.15E08	1.9	7530	[25]
(37)	$C_2H_6+O=C_2H_5+OH$	8.98E07	1.92	5690	[25]
(38)	$C_2H_6+OH=C_2H_5+H_2O$	3.54E06	2.12	870	[25]
(39)	$C_2H_6+CH_3=C_2H_5+CH_4$	6.14E06	1.74	10450	[25]
(40)	$C_2H_5+H+M=C_2H_6+M$ H_2/2./H_2O/6./CH_4/2./CO/1.5/CO_2/2./C_2H_6/3./Ar/0.7/	5.21E17	–0.99	1580	[25]
(41)	$C_2H_5+H=C_2H_4+H_2$	2.00E12	0.0	0	[25]
(42)	$C_2H_5+O=CH_3+CH_2O$	1.32E14	0.0	0	[25]
(43)	$C_2H_5+O_2=C_2H_4+HO_2$	8.40E11	0.0	3875	[25]
(44)	$C_2H_4+H+M=C_2H_5+M$ H_2/2./H_2O/6./CH_4/2./CO/1.5/CO_2/2./C_2H_6/3./Ar/0.7/	1.08E12	0.45	1820	[25]
(45)	$C_2H_4+H=C_2H_3+H_2$	1.33E06	2.53	12240	[25]

Table 2. Continued

No.	Reaction	*A*	*n*	E_a	ref
(46)	$C_2H_4+O=CH_3+HCO$	1.92E07	1.83	220	[25]
(47)	$C_2H_4+OH=C_2H_3+H_2O$	3.60E06	2.0	2500	[25]
(48)	$C_2H_4+M=C_2H_2+H_2+M$ H_2/2./H_2O/6./CH_4/2./CO/1.5/CO_2/2./C_2H_6/3./Ar/0.7/	8.00E12	0.44	88770	[25]
(49)	$C_2H_4+CH_3=C_2H_3+CH_4$	2.27E05	2.0	9200	[25]
(50)	$C_2H_3+H+M=C_2H_4+M$ H_2/2./H_2O/6./CH_4/2./CO/1.5/CO_2/2./C_2H_6/3./Ar/0.7/	6.08E12	0.27	280	[25]
(51)	$C_2H_3+H=C_2H_2+H_2$	3.00E13	0.0	0	[25]
(52)	$C_2H_3+O=CH_2CO+H$	3.00E13	0.0	0	[25]
(53)	$C_2H_3+OH=C_2H_2+H_2O$	5.00E12	0.0	0	[25]
(54)	$C_2H_3+O_2=HCO+CH_2O$	3.98E12	0.0	–240	[25]
(55)	$C_2H_2+H+M=C_2H_3+M$ H_2/2./H_2O/6./CH_4/2./CO/1.5/CO_2/2./C_2H_6/3./Ar/0.7/	5.60E12	0.0	2400	[25]
(56)	$C_2H_2+O=CO+CH_2$	1.02E07	2.0	1900	[25]
(57)	$C_2H_2+O=OH+C_2H$	4.60E19	–1.41	28950	[25]
(58)	$C_2H_2+O=H+HCCO$	1.02E07	2.0	1900	[25]
(59)	$C_2H_2+OH=CH_2CO+H$	2.18E-4	4.5	–1000	[25]
(60)	$C_2H_2+OH=H+HCCOH$	5.04E05	2.3	13500	[25]
(61)	$C_2H_2+OH=C_2H+H_2O$	3.37E07	2.0	14000	[25]
(62)	$C_2H_2+OH=CH_3+CO$	4.83E-4	4.0	–2000	[25]
(63)	$C_2H+O=CH+CO$	5.00E13	0.0	0	[25]
(64)	$C_2H+OH=H+HCCO$	2.00E13	0.0	0	[25]
(65)	$CH_3O+H+M=CH_3OH+M$ H_2/2./H_2O/6./CH_4/2./CO/1.5/CO_2/2./C_2H_6/3./	5.00E13	0.0	0	[25]
(66)	$CH_3O+H=H+CH_2OH$	3.40E06	1.6	0	[25]
(67)	$CH_3O+H=H_2+CH_2O$	2.00E13	0.0	0	[25]
(68)	$CH_3O+H=OH+CH_3$	3.20E13	0.0	0	[25]
(69)	$CH_3O+O=OH+CH_2O$	1.00E13	0.0	0	[25]
(70)	$CH_3O+OH=H_2O+CH_2O$	5.00E12	0.0	0	[25]
(71)	$CH_3O+O_2=HO_2+CH_2O$	4.28E-13	7.6	–3530	[25]
(72)	$CH_2O+OH=HCO+H_2O$	3.00E13	0.0	1200	[26]
(73)	$CH_2O+HO_2=HCO+H_2O_2$	4.40E06	2.0	12000	[26]
(74)	$HCO+M=CO+H+M$ CH_4/3./H_2O/5./CO_2/3./CO/2./H_2/2./	2.50E14	0.0	16800	[23]
(75)	$HCO+H=CO+H_2$	2.16E14	0.0	0	[26]
(76)	$HCO+H+M=CH_2O+M$ H_2O/5./CO_2/3./CO/2./H_2/2./	6.56E14	0.0	–8659	[26]
(77)	$HCO+O_2=CO+HO_2$	4.22E13	0.0	1700	adjusted
(78)	$HCO+O=CO+OH$	3.00E13	0.0	0	[26]
(79)	$HCO+HCO=CH_2O+CO$	4.50E13	0.0	0	[26]
(80)	$CO+OH=CO_2+H$	4.40E06	1.5	–700	[26]
(81)	$CO+HO_2=CO_2+OH$	1.50E14	0.0	23600	[26]
(82)	$CO+O+M=CO_2+M$ CH_4/3./H_2O/5./CO_2/3./CO/2./H_2/2./	6.17E14	0.0	3002	[23]
(83)	$H+O_2=OH+O$	1.20E17	–0.91	16500	[26]
(84)	$H+O_2+M=HO_2+M$ H_2/3./H_2O/21./O_2/0./CO_2/5./CO/2./	3.61E17	–0.72	0	[23]
(85)	$O+H_2=OH+H$	1.50E07	2.0	7600	[26]
(86)	$H+O+M=OH^*+M$	1.20E13	0.0	6930	[26]
(87)	$OH^*+M=OH+M$	5.20E10	0.5	0	[26]
(88)	$OH^*+H_2O=OH+H_2O$	8.60E12	0.5	0	[26]
(89)	$OH^*+H_2=OH+H_2$	1.50E12	0.5	0	[26]
(90)	$OH^*+H=OH+H$	1.50E12	0.5	0	[26]
(91)	$OH^*+O_2=OH+O_2$	1.50E12	0.5	0	[26]

Table 2. Continued

No.	Reaction	*A*	*n*	E_a	ref
(92)	OH*+O=OH+O	1.50E12	0.5	0	[26]
(93)	OH*+OH=OH+OH	1.50E12	0.5	0	[26]
(94)	OH*=OH+hν hν /3064/	1.40E06	0.0	0	[26]
(95)	OH+M=H+O+M	1.10E17	−0.6	102490	[23]
(96)	OH+H_2=H_2O+H	1.00E08	1.6	3300	[26]
(97)	OH+OH=H_2O+O	1.50E09	1.14	0	[26]
(98)	H+H+M=H_2+M H_2O/0./CO_2/0./H_2/0./	6.40E17	−1.0	0	[26]
(99)	O_2+M=O+O+M H_2O/5./	1.20E14	0.0	107800	[23]
(100)	OH+H+M=H_2O+M H_2O/5./	7.50E23	−2.6	0	[23]
(101)	H+HO_2=OH+OH	1.50E14	0.0	1000	[26]
(102)	H+HO_2=H_2+O_2	1.00E14	0.0	700	[26]
(103)	O+HO_2=OH+O_2	2.00E13	0.0	0	[26]
(104)	OH+HO_2=H_2O+O_2	2.00E13	0.0	0	[26]
(105)	HO_2+HO_2=H_2O_2+O_2	2.00E12	0.0	0	[26]
(106)	H+H_2O_2=H_2O+OH	1.00E13	0.0	3600	[26]
(107)	O+H_2O_2=OH+HO_2	2.80E13	0.0	6400	[26]
(108)	OH+H_2O_2=H_2O+HO_2	7.00E12	0.0	1400	[26]
(109)	H_2O_2+M=OH+OH+M	1.20E17	0.0	45500	[26]
(110)	H_2O_2+H=H_2+HO_2	5.01E13	0.0	7900	[26]

Rate constants are expressed in the form $k=AT^n \exp(-E_a/RT)$ where units are mol, m^{-3}, s, K and cal·mol^{-1}. Reversed reactions were automatically included in the computer program through equilibrium constants computed from polynomial fits to thermodynamical data.

below 2000 K, the excited OH radical was found to be formed mainly in the following reaction[18]

$$H + O + M = OH^* + M \quad (86)$$

($\Delta H = -104.3$ kcal at 1000 K). The excited OH radical may loose its energy nonradiantly through collisions with some chemical species or radiantly by emitting the 306.4 nm photon:

$$OH^* = OH + h\nu \quad (94)$$

We examined the excitation and de-excitation steps of the OH radical in the mechanism scheme.

The final reaction scheme for ignition of acetaldehyde-oxygen mixtures diluted in Ar consists of 110 elementary reactions involving 34 species and is listed in Table 2. The calculated values for the ignition delay times for all mixtures studied are shown as lines in the corresponding figures. As shown in Figure 2, there is good agreement between the calculated and the experimental values for mixtures E and G with Φ=1. As the equivalence ratio increases over Φ=1, the calculated values become shorter and shorter than the corresponding observed values. Contrary, for the fuel-lean mixture (mixture A), the calculated values are longer than the corresponding observed values. These deviations are due to that acetaldehyde and oxygen play roles as an inhibitor and a promoter, respectively. A sensitivity analysis was performed to identify significant reactions in the acetaldehyde oxidation. To determine the sensitivity of each reaction to the ignition delay time, one must find out how the rate constant of a given elementary reaction give rise to an effect on the calculated ignition delay time. Defining the sensitivity as $(\tau'-\tau)/\tau \times 100$ where τ' and τ are the calculated delay times from after and before the change in rate constant, a computer simulation was performed for mixture G, by multiplying rate constant of a given reaction from Table 2 by 5 or 1/5. The sensitivity spectrum, shown in Figure 4, confirms that the oxidation acetaldehyde is initiated via rupture of C-C bond

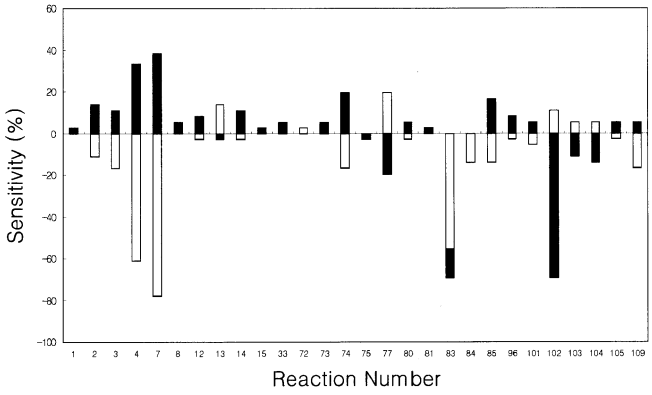

Figure 4. Sensitivity spectrum of ignition delay time in mixture G at 1499 K. The solid and open bars represent the results of multiplying the indicated rate constants by 5 and 1/5, respectively. The numbers indicate the reaction number in Table 2.

$$CH_3CHO + M = CH_3 + HCO + M \quad (2)$$

rather than the abstraction of H atom:

$$CH_3CHO + M = CH_3CO + H + M \quad (1)$$

The chain reaction is promoted by the attack of H, OH and HO_2 radicals to form acetyl radical:

$$CH_3CHO + H = CH_3CO + H_2 \quad (3)$$

$$CH_3CHO + OH = CH_3CO + H_2O \quad (4)$$

$$CH_3CHO + HO_2 = CH_3CO + H_2O_2 \quad (7)$$

These reactions, which consume H, OH and HO_2 have a strong effect on acetaldehyde oxidation ignition. The reactions of CH_3CHO with OH and HO_2 are the main propagation steps, while the decomposition of CH_3CO to CH_2CO supplies additional H atoms to promote reactions (83) and (102).

Our oxidation mechanism is represented schematically in Figure 5. Most part of acetaldehyde become to CH_2CO through H-atom abstraction channels. The C-C bond breaking occurs through two dissociative attacks of O atoms and OH radicals. The attack of O atoms on CH_2CO forms two equivalent ratio of HCO radical, while the attack of OH radicals produces CH_2O and HCO radicals. The most striking features in the acetaldehyde oxidation are the chain propagation reactions generated by HCO:

$$HCO + M = CO + H + M \quad (74)$$

$$HCO + O_2 = CO + HO_2 \quad (77)$$

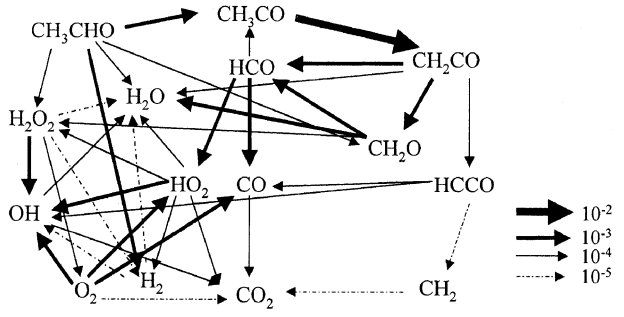

Figure 5. Pathway diagram showing oxidation routes of CH_3CHO. The values represent molar production rates (mol cm^{-3} s^{-1}) at τ = 310 μs and T=1499 K.

The sensitivity spectrum shows that these reactions moderately affect the ignition delay time of the acetaldehyde oxidation. The decomposition of HCO subsequent to reaction (2) supplies H radical in the high-temperature region in part and promotes the production of OH radical *via* the reaction of H atom with oxygen molecule:

$$H + O_2 = OH + O \quad (83)$$

Reaction (83) is one of the most important branching chain reactions in the oxidation of hydrocarbon fuels, since the 80% of oxygen molecule is consumed *via* this reaction. This reaction, however, competes strongly with the reaction between H atom with HO_2 radical:

$$H + HO_2 = H_2 + O_2 \quad (102)$$

The sensitivity spectrum shows that ignition is very sensitive to reactions of hydroperoxyl radical producing H_2, O_2 or H_2O and decomposition of H_2O_2.

Conclusions

This shock tube study of CH_3CHO-O_2-Ar behind a reflected shock reveals the ignition kinetics of the acetaldehyde oxidation. The experimental data match the mechanism scheme consisting of 110 elementary steps well. The decomposition of acetaldehyde into HCO and CH_3 might initiate the oxidation of acetaldehyde. The elementary steps associated with the decomposition and oxidation of HCO play a key role in ignition. The main propagation steps involving CH_3CHO are the reactions with OH and HO_2. The mechanism of acetaldehyde oxidation at high temperature is quite different from those for cool flame phenomena at low temperature, in which the acetaldehyde oxidation has been characterized by the rate of branching through formation of hydroperoxides, such as CH_3CO_3H and CH_3OOH.

Acknowledgment. This work was financially supported by the Basic Science Research Institute Program of the Ministry of Education, 1994-1999 Project NO. BSRI-98-3432.

References

1. Kaiser, E. W.; Westbrook, C. K.; Pitz, W. J. *Int. J. Chem. Kinet*. **1986**, *18*, 655.
2. Pugh, S. A.; Kim, H.-R.; Ross, J. *J. Chem. Phys.* **1987**, *86*, 776.
3. Cavanagh, J.; Cox, R. A.; Olson, G. *Combust. Flame* **1990**, *82*, 15.
4. Kojima, S. *Combust. Flame* **1994**, *99*, 87.
5. Colket, M. B. III; Naeceli, D. W.; Glassman, I. In *Proceedings of the 16th Symp. (Int.) on Combustion*; The Combustion Institute: 1977; p 1023.
6. Dagaut, P.; Reuillon, M.; Voisin, D.; Cathonnet, M.; McGuinness, M.; Simmie, J. M. *Combust. Sci. Tech*. **1995**, *107*, 301.
7. Ranzi, E.; Sogaro, A.; Gaffuri, P.; Pennati, G.; Westbrook, C. K.; Pitz, W. J. *Combust. Flame* **1994**, *99*, 201.
8. Beeley, P.; Criffiths, J. F.; Hunt, B. A.; Williams, A. In *Proceedings of the 16th Symp. (Int.) on Combustion*; The Combustion Institute: 1977; p 1013.
9. Hidaka, Y.; Syga, M. *Mass. Spectrosc*. **1987**, *35*, 74.
10. Kang, J.-G.; Ryu, J.-C.; Choi, E. S.; Kang, S. K.; Yeo, H.-G. *Combust. Flame* **1996**, *106*, 81.
11. Ryu, J.-C. ; Seo, H.; Kang, J.-G.; Oh, K.-H. *Bull. Korean Chem. Soc*. **1997**, *18*, 1071.
12. Gordon, S.; McBride, B. J. *Computer Program for Calculation of Complex Chemical Equilbrium Compositions, Rocket Performance, Incident and Reflected Shocks, and Chapman-Jouguet Detonations*, NASA SP-273; 1971.
13. Kee, R. J.; Rupley, F. M.; Miller, J. A. *Chemkin-II: A Fortran Chemical Kinetics Package for the Analysis of Gas Phase Chemical Kinetics*, SAND89-8009B; 1989.
14. Turanyl, T. *KINALC: CHEMKIN Based Program for Kinetic Analysis*; 1996.
15. Yoon, H.-M.; Yeo, H.-G.; Yun, S. S.; Kim, C.-S.; Kang, J.-G. *Combust. Flame* **1993**, *92*, 481.
16. Benson, S. W. *The Foundations of Chemical Kinetics*; McGraw-Hill: New York, 1960; p 380.
17. Gaydon, A. G. *The Spectroscopy of Flames*; Chapman and Hall: London, 1974; pp 266-269.
18. Hidaka, Y.; Takahashi, S.; Kawano, H.; Suga, M.; Gardiner, W. G. Jr. *J. Phys. Chem.* **1982**, *89*, 3109.
19. Kern, R. D.; Singh, H. J.; Xie, K. In *Proceedings of the 17th Symp. (Int.) on Shock Wave and Shock Tubes*; American Institute of Physics: 1989; p 487.
20. Lifshitz, A.; Ben-Hamou, H. *J. Phys. Chem*. **1983**, *87*, 1782.
21. Dagaut, P.; Boettner, J.-C.; Cathonnet, M. *Combust. Sci. Tech*. **1991**, *77*, 127.
22. Drake, M. C.; Blint, R. J. *Combust. Sci. Tech.* **1991**, *75*, 261.
23. Lee, K. Y.; Yang, M. H.; Puri, I. K. *Combust. Flame* **1993**, *92*, 419.
24. Karra, S. B.; Gutman, D.; Senkan, S. M. *Combust. Sci. Tech*. **1988**, *60*, 45.
25. Smith, G. P.; Golden, D. M.; Frenklach, M.; Moriarty, N. W.; Eiteneer, B.; Goldenberg, M.; Bowman, C. T.; Hanson, R. K.; Song, S.; Gardiner, W. C. Jr., Lissianski, V. V.; Qin, Z. *http://www.me. Berkeley.edu /gri_mech*.
26. Hidaka, Y.; Taniguchi, T.; Tanaka, H.; Kamesawa, T.; Inami, K.; Kawano, H. *Combust. Flame* **1993**, *92*, 365.